Inorg. Chem. **1985**, *24*, 2900–2905

the paramagnetic $U(BH_3CH_3)_4$. While the analogous uranium dimers have not yet been reproducibly isolated, a 1:1 mixture of $U(BH_3CH_3)_4$ and THF can be probed by NMR to determine what possible species exist in solution. The low-temperature ^1H NMR spectrum of $U(BH_3CH_3)_4$ and 1 equiv of THF in toluene-d_8 is reported in Table VII. At low temperatures (<−30 °C), peaks with chemical shifts identical with those of authentic compounds can be observed for $U(BH_3CH_3)_4$ and $U(BH_3CH_3)_4 \cdot 2THF$.[14] In addition, a third species is present, having integrated intensities 12:12:4:4—$U(BH_3CH_3)_4 \cdot THF$. There is no evidence (down to −96 °C) for inequivalent methyltrihydroborate sites, and so $U(BH_3CH_3)_4 \cdot THF$ is probably monomeric in solution. K_{eq} (by integration) for the reaction

$$U(BH_3CH_3)_4 + U(BH_3CH_3)_4 \cdot 2THF \rightleftarrows 2U(BH_3CH_3)_4 \cdot THF$$

is ~20 at −80 °C. This indicates that the dimers isolated in the solid state are likely to have a more complex solution state.

Upon mixing equimolar amounts of $U(BH_3CH_3)_4$ and $Th(BH_3CH_3)_4$ in toluene-d_8 and recording the ^1H variable-temperature NMR spectra, we observe well-resolved peaks for both the Th and U compounds at low temperatures. As the solution temperature is raised, the BH_3 peaks broaden and the CH_3 peaks coalesce, becoming one time-averaged signal. The observed rate is concentration dependent. If under identical conditions Zr is substituted for Th (decreasing the ionic radius by 0.15 Å), no exchange is observed up to 80 °C. The resultant chemical shift of the Th/U exchange process is the weighted average of the individual species (within experimental error). These observations are consistent with an associative BH_3CH_3 exchange process and suggest that rapid methyltrihydroborate site exchange via a transient dimeric species is a plausible explanation for the lack of inequivalent sites observed in the NMR spectra of the diamagnetic thorium dimers.

Acknowledgment. This work was supported by the Director, Office of Energy Research, Office of Basic Energy Sciences, Chemical Sciences Division of the U.S. Department of Energy, under Contract No. DE-AC03-76SF00098.

Registry No. $[Th(BH_3CH_3)_4]_2 \cdot OEt_2$, 97295-99-3; $[Th(BH_3CH_3)_4 \cdot THF]_2$, 97296-00-9.

Supplementary Material Available: Lists of anisotropic thermal parameters, distance restraints on H atoms, hydrogen positional and thermal parameters, H atom distances, and observed structure factors (33 pages). Ordering information is given on any current masthead page.

---

[14] Shinomoto, R., unpublished results.

Contribution from the Department of Chemistry, Washington State University, Pullman Washington 99164,
Istituto di Chimica delle Macromolecole del CNR, Milano, Italy,
Istituto di Chimica Generale e Inorganica, Università di Modena, Modena, Italy,
and Istituto Chimico, Facoltà di Ingegneria, Università di Bologna, Bologna, Italy

Crystal Structure and Spectroscopic, Magnetic, and Electrical Properties of a Copper(II) Dimer, Melaminium Hexachlorodicuprate(II), Exhibiting a New Stacking Interaction

A. COLOMBO,[1a] L. MENABUE,[1b] A. MOTORI,[1c] G. C. PELLACANI,*[1b] W. PORZIO,[1a] F. SANDROLINI,[1c] and R. D. WILLETT[1d]

Received October 8, 1984

The $(C_3N_6H_8)Cu_2Cl_6$ compound ($C_3N_6H_8$ = melaminium dication, hereafter abbreviated as melH$_2$) has been synthesized and its crystal structure determined. A number of its physical properties were examined, including its electronic and vibrational spectra, as well as magnetic and electrical behavior. The crystals are monoclinic, space group $P2_1/c$, with $a = 6.6600$ (1) Å, $b = 10.0598$ (2) Å, $c = 19.2691$ (12) Å, $\beta = 96.011$ (3)°, $Z = 4$, $d_{calcd} = 2.42$ g·cm^{-3}, and $d_{measd} = 2.45$ g·cm^{-3}. The structure, solved by direct methods and refined by least-squares calculations to $R = 3.9\%$, consists of melaminium dications and $Cu_2Cl_6^{2-}$ dimers stacked to form infinite chains in a manner not previously observed. The coordination of the copper atoms may be described as distorted square pyramidal. Electronic and vibrational results are discussed on the basis of the crystal structure. The compound exhibits predominantly antiferromagnetic exchange interactions. An intradimer singlet–triplet energy splitting of $\Delta E/k = 54$ K is deduced, with weaker ferromagnetic coupling between dimers. A comparison with the magnetic behavior of other $Cu_2Cl_6^{2-}$ dimers is given. Electrical conductivity measurements classify the compound as an insulating material.

Introduction

The copper(II) ion plays a significant role in transition-metal chemistry, impacting on such areas as catalysis, bioinorganic chemistry, magnetic interactions, electrical conductors in solids, etc. The stereochemistry of the copper(II) ion is certainly the most rich among the ionic transition-metal complexes. Even with the simple halide ligands, a nearly continuous range of stereochemistries is obtained. This "softness" of the copper(II) coordination sphere has allowed the systematic exploration of the magnetostructural correlations covering a wide range of structural parameters. These correlations have been successfully applied to the synthesis of a large number of low-dimensional magnetic systems. It appears that many aspects of these variations in coordination geometry can be largely rationalized on the basis of a balance between crystal field stabilization and electrostatic effects. In the case of A_nCuX_{2+n} type systems, where A is an organic ammonium cation, the electrostatic effects are modulated by the precise nature of the organic groups. This has been noted in a recent review of the structures of $ACuCl_3$ salts.[2] Three classes of structures were observed: (1) isolated $Cu_2Cl_6^{2-}$ dimers; (2) $Cu_2Cl_6^{2-}$ dimers stacked to form chains; (3) uniform $(CuCl_3)_n^{n-}$ chains. The first class occurs with large cations with little or no hydrogen-bonding capabilities. The last two classes occur with small and/or strong hydrogen-bonding cations. For class 2, a simple graphic representation of the packing of the $Cu_nX_{2n+2}^{2-}$ polymers has been given, and a nomenclature has been developed.[3] A large number of permutations of stacking patterns for the

---

(1) (a) Istituto di Chimica delle Macromolecule del CNR. (b) Università di Modena. (c) Università di Bologna. (d) Washington State University.

(2) Willett, R. D.; Geiser, U. *Croat. Chem. Acta*, in press, and references cited therein.

(3) (a) Willett, R. D.; Geiser, U. XIII International Union of Crystallography Congress, Hamburg, 1984. (b) Geiser, U.; Willett, R. D.; Lind, M.; Emerson, K., to be submitted for publication in *Inorg. Chem.*

0020-1669/85/1324-2900$01.50/0

various polymers appear to be possible, and the actual crystal chemistry may be much more complex than previously suspected. Thus these systems allow the practice of what has been called "crystal lattice engineering"[4] to a specific class of mixed organic–inorganic materials that exhibit a wide variety of interesting properties. The study of the title compound was initiated as part of this program to study the interactions of protonated amines with copper halides. The particular amine selected, melamine [$C_3N_3(NH_2)_3$, I], was chosen because, containing six nitrogen atoms, it can form very extensive hydrogen bonds.

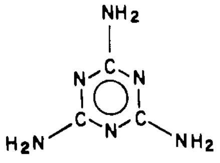

I

The synthesis and crystal structure of $(melH_2)Cu_2Cl_6$ are reported herein, as well as the investigations of a number of its physical properties including electronic and vibrational spectra and its magnetic and electrical behavior.

Experimental Section

Preparation of Melaminium Hexachlorodicuprate(II), $(melH_2)Cu_2Cl_6$. The compound was prepared by mixing the amine and the copper(II) chloride dihydrate salt in any stoichiometric ratio in concentrated hydrogen chloride. When the mixture was allowed to stand for some hours, red crystals precipitated. Anal. Calcd for $C_3H_8Cu_2N_6Cl_6$: C, 7.69; H, 1.72; N, 17.96; Cl, 45.46. Found: C, 7.71; H, 1.74; N, 17.91; Cl, 45.66.

Physical Measurements. The electronic spectra of the solid compound were recorded as Nujol mull transmission spectra with a SHIMADZU MPS 50L spectrophotometer. The infrared spectra as Nujol mulls on polythene as support (500–60 cm^{-1}) were recorded with a Perkin-Elmer 180 spectrophotometer. Thermogravimetric and differential scanning calorimetric (DSC) analyses were performed with METTLER TA 3000 and Perkin-Elmer DSC-1 instruments, respectively. Magnetic susceptibility measurements were made on a PAR vibrating-sample magnetometer at Washington State University in the temperature range 80–300 K and at Clark University in the temperature range 1.6–80 K, in an applied field of 10 kOe. Diamagnetic correction (-184×10^{-6} emu/mol of dimers) and TIP correction (120×10^{-6} emu/mol of dimers) were made.

Electrical Measurements. Disks of 28 mm in diameter and variable thicknesses (up to 2 mm) suitable for the electrical measurements were compacted in vacuo under a pressure of 0.2 kN/mm^2. The samples were then sintered at 150 °C in vacuo in order to minimize intergranular effects and stabilize the material for the subsequent electrical measurements. Higher temperatures were found to cause irreversible changes in the compound. Since preliminary measurements pointed out insulating properties of the material at room temperature, a three-terminal technique was used for electrical measurements. The voltmeter–ammeter method in dc (direct current) and bridge method in ac (alternating current) measurements were used with the cell and instrumentation described elsewhere.[5-8] The samples were first coated with gold by vacuum evaporation, and then measurements were made from 140 °C to room temperature to avoid effects of casual gas or vapor adsorption on the sample surfaces. Dc measurements were made at a constant electrical field of 1 $kV\cdot cm^{-1}$. Both charging and discharging currents were measured in order to notice possible relaxation processes in the ultralow-frequency range,[8-11] usually due to structural effects in materials.

Crystallographic Data Collection and Structure Determination and Refinement. A roughly cubic crystal, ca. 0.1 mm^3 in size, sealed in a low-absorption glass capillary, was used for X-ray measurements. Unit cell parameters and integrated intensities were measured by use of a Philips PW-1100 single-crystal automatic diffractometer. Unit cell and crystal symmetries were determined by use of the standard control program of the PW1100 system[12] with a randomly oriented crystal; cell parameters and their esd's. were refined by least-squares methods from the accurate positioning of 56 strong reflections. Crystal data and working conditions for the integrated intensities measurements are reported in Table I. Intensities were corrected for Lorentz and polarization effects but not for absorption in view of the crystal size. The intensities of two standard reflections showed a light decay (<15%) during the data collection; correction was applied. The structure was solved by direct methods, with the set of programs prepared by A. Colombo, based on a probability distribution for the structure factor signs in centrosymmetric crystals.[13] From four equivalent solutions, the best phase distribution was selected by a figure of merit.[14] From the subsequent E map and the use of 402 reflections, the Cu and Cl atoms were located. An electron density map gave the positions of all the remaining non-hydrogen atoms.

Table I. Crystal Data and Working Conditions

$Cu_2Cl_6N_6C_3H_8$
mol wt = 467.94
space group $P2_1/c$ (no. 14)
$a = 6.6600$ (1) Å
$b = 10.0598$ (2) Å
$c = 19.2691$ (12) Å

$V = 1283.9$ Å^3
$Z = 4$
$d_{calcd} = 2.42$ $g\cdot cm^{-3}$
$\beta = 96.011$ (3)°
$F(000) = 912$ e/cell
$\mu_{Mo\ K\alpha} = 46.52$ cm^{-1} [a]

scan mode: ω–2θ
scan speed: 2.4° min^{-1}
scan width: 1.2°
θ range (d_{min}) 2–28° (0.76 Å)
measd reflcs: $\pm h,+k,+l$
no. of collcd reflections: 3278
no. of obsd reflcs[b] (with $I > 3.0\sigma(I)$): 2206
std reflcs: 2 (measd every 110 reflcns)
wavelength (Mo Kα graphite-monochromated radiation): 0.7107 Å
approx cryst size (roughly cubic): 0.1 × 0.1 × 0.1 mm
temp: 20 °C

[a] The variation in transmittance was estimated at ±3.5%. [b] $\sigma(I)$ = (peak counts + total background counts)$^{1/2}$.

Table II. Atomic Fractional Coordinates of $Cu_2Cl_6N_6C_3H_8$, with Esd's in Parentheses.[a]

atom	x/a	y/b	z/c
Cu(1)	32906 (12)	44050 (8)	41367 (4)
Cu(2)	16636 (11)	38457 (8)	57605 (4)
Cl(1)	45089 (22)	62363 (16)	36334 (7)
Cl(2)	25309 (22)	56456 (15)	50844 (7)
Cl(3)	23981 (22)	25825 (15)	48004 (7)
Cl(4)	39670 (24)	30544 (16)	32612 (8)
Cl(5)	5570 (22)	52818 (16)	65375 (7)
Cl(6)	4928 (23)	20287 (16)	62851 (7)
N(1)	1575 (8)	8643 (6)	6085 (2)
N(2)	4510 (8)	9913 (5)	5950 (2)
N(3)	3354 (8)	9558 (5)	7059 (2)
N(4)	2608 (9)	9030 (6)	5001 (3)
N(5)	448 (9)	8354 (6)	7176 (3)
N(6)	6322 (8)	10682 (6)	6952 (3)
C(1)	2920 (9)	9209 (6)	5678 (3)
C(2)	4741 (9)	10053 (6)	6640 (3)
C(3)	1784 (9)	8840 (6)	6785 (3)

[a] The values are $\times 10^5$ for Cu and Cl atoms and $\times 10^4$ for N and C atoms.

The positional and thermal parameters were refined by block-diagonal-matrix least-squares methods with unitary weight factors to a conventional $R = 0.080$ (4 isotropic cycles) and $R = 0.039$ (4 anisotropic cycles) for the 2206 observed reflections. At this R value convergence was achieved (final shift-to-error ratio <0.1). No hydrogen atoms were located from the subsequent difference electron density map.

Atomic scattering factors were taken from ref 15; both real and imaginary components of the anomalous dispersion[15] were included.

---

(4) Arend, H. *Proc. Int. Summer Sch. Cryst. Growth Mater. Res.* **1983**.
(5) Sandrolini, F.; Manaresi, P. *J. Polym. Sci., Polym. Chem. Ed.* **1976**, *14*, 939.
(6) Sandrolini, F.; Cremonini, P. *Mater. Plast. Elastomeri* **1979**, 405.
(7) Sandrolini, F. *J. Phys. E* **1980**, *13*, 152.
(8) Menabue, L.; Pellacani, G. C.; Battaglia, L. P.; Bonamartini Corradi, A.; Sandrolini, F.; Motori, A.; Pylkki, R. J.; Willett, R. D. *J. Chem. Soc. Dalton Trans.* **1984**, 2187.
(9) Hamon, B. *Proc. IEEE* **1952**, *99*, 151.
(10) Baird, M. E. *Rev. Mod. Phys.* **1968**, *40*, 219.
(11) Shthraus, V. D. *Mekh. Polim.* **1976**, *12*, 507.
(12) "User Manual for PW1100 Philips"; Philips: Eindhoven, The Netherlands.
(13) Allegra, G. *Acta Crystallogr.* **1965**, *19*, 949.
(14) Allegra, G.; Colombo, A. *Acta Crystallogr., Sect. A: Cryst. Phys., Diffr., Theor. Gen. Crystallogr.* **1974**, *A30*, 727.
(15) "International Tables for X-ray Crystallography"; Kynoch Press: Birmingham, England, 1974; Vol. IV, pp 99–100 and 149–150.

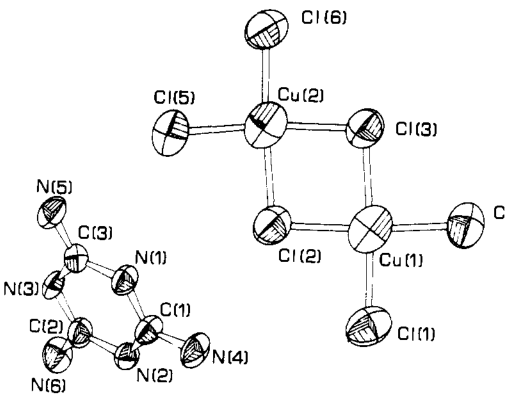

Figure 1. Diprotonated melamine–hexachlorodicuprate molecule viewed perpendicularly to the four-membered-ring plane.

Table III. Selected Bond Distances (Å) and Bond Angles (deg) with Esd's in Parentheses for the $Cu_2Cl_6^{2-}$ Anion Chain[a]

Cu(1)–Cl(1)	2.271 (2)	Cu(2)–Cl(2)	2.338 (2)
Cu(1)–Cl(2)	2.311 (2)	Cu(2)–Cl(3)	2.338 (2)
Cu(1)–Cl(3)	2.347 (2)	Cu(2)–Cl(5)	2.259 (2)
Cu(1)–Cl(4)	2.248 (2)	Cu(2)–Cl(6)	2.266 (2)
Cu(1)$^{\mathrm{II}}$–Cl(5)$^{\mathrm{III}}$	2.767 (2)	Cu(2)–Cl(1)$^{\mathrm{II}}$	2.692 (2)
Cu(1)–Cl(2)–Cu(2)	96.3 (1)	Cu(1)–Cl(1)–Cu(2)$^{\mathrm{II}}$	98.9 (1)
Cu(1)–Cl(3)–Cu(2)	95.3 (1)	Cu(2)$^{\mathrm{II}}$–Cl(5)$^{\mathrm{II}}$–Cu(1)$^{\mathrm{III}}$	96.4 (1)
Cl(1)–Cu(1)–Cl(2)	91.0 (1)	Cl(1)$^{\mathrm{II}}$–Cu(1)$^{\mathrm{II}}$–Cl(5)$^{\mathrm{III}}$	93.6 (1)
Cl(1)–Cu(1)–Cl(3)	171.3 (1)	Cl(2)$^{\mathrm{II}}$–Cu(1)$^{\mathrm{II}}$–Cl(5)$^{\mathrm{III}}$	92.3 (1)
Cl(1)–Cu(1)–Cl(4)	93.5 (1)	Cl(3)$^{\mathrm{II}}$–Cu(1)$^{\mathrm{II}}$–Cl(5)$^{\mathrm{III}}$	94.0 (1)
Cl(2)–Cu(1)–Cl(3)	84.4 (1)	Cl(4)$^{\mathrm{II}}$–Cu(1)$^{\mathrm{II}}$–Cl(5)$^{\mathrm{III}}$	88.0 (1)
Cl(2)–Cu(1)–Cl(4)	175.5 (1)	Cl(2)–Cu(2)–Cl(1)$^{\mathrm{II}}$	89.3 (1)
Cl(2)–Cu(2)–Cl(3)	84.0 (1)	Cl(3)–Cu(2)–Cl(1)$^{\mathrm{II}}$	93.4
Cl(2)–Cu(2)–Cl(5)	89.5 (1)	Cl(5)–Cu(2)–Cl(1)$^{\mathrm{II}}$	95.3 (1)
Cl(2)–Cu(2)–Cl(6)	171.8 (1)	Cl(6)–Cu(2)–Cl(1)$^{\mathrm{II}}$	97.8 (1)
Cl(3)–Cu(1)–Cl(4)	91.1 (1)		
Cl(3)–Cu(2)–Cl(5)	169.1 (1)		
Cl(3)–Cu(2)–Cl(6)	91.4 (1)		
Cl(5)–Cu(2)–Cl(6)	94.0 (1)		

[a] Three superimposed molecules in the chain are taken into account; the atoms of the second and the third molecule are quoted with II and III, respectively.

All the calculations were performed on the UNIVAC 1100/80 of the Consorzio Interuniversitario Lombardo per l'Elaborazione Automatica at Milan.

Table II reports the final positional parameters for the 17 independent atoms with their estimated standard deviations. Corresponding anisotropic thermal vibration parameters and lists of observed and calculated structure factors are deposited in the supplementary material.

Results and Discussion

The reaction between melamine and $CuCl_2 \cdot 2H_2O$ at any stoichiometric ratio in concentrated hydrogen chloride gives rise only to the formation of a compound of formula $(melH_2)Cu_2Cl_6$, stable in air up to 473 K, as demonstrated by TG and DSC analyses.

Description of the Structure. The crystal structure consists of $N_6C_3H_8^{2+}$ dications and infinite $(Cu_2Cl_6^{2-})_n$ chains running along the short *a* axis. A projection of the asymmetric unit in the cell, $N_6C_3H_8^{2+}Cu_2Cl_6^{2-}$ viewed along a direction orthogonal to the least-squares plane through the bridged heavy atoms, is shown in Figure 1 together with the atom-numbering scheme.

The anionic part of the structure can be described as noncentrosymmetric $Cu_2Cl_6^{2-}$ dimers related to each other by the crystallographic inversion centers and stacked to form infinite chains along *a* (the identity period being 6.66 Å). This leads to a basic five-coordination of the copper (see below) with two significant Cu–Cl bonds between adjacent dimers. As may be seen from Figure 2, these long bonds involve two "cis" terminal chlorines in each dimer, one linking the upper and the other linking the lower dimer by two nonequivalent Cu atoms. The bond lengths shown by dashed lines in Figure 2 are 2.692 Å for Cu(2)–Cl(1)$^{\mathrm{II}}$ and 2.767 Å for Cu(1)$^{\mathrm{II}}$–Cl(5)$^{\mathrm{III}}$ (see also Table III), while the distances between the least-squares planes of adjacent dimers are 3.21 and 3.08 Å alternatively.

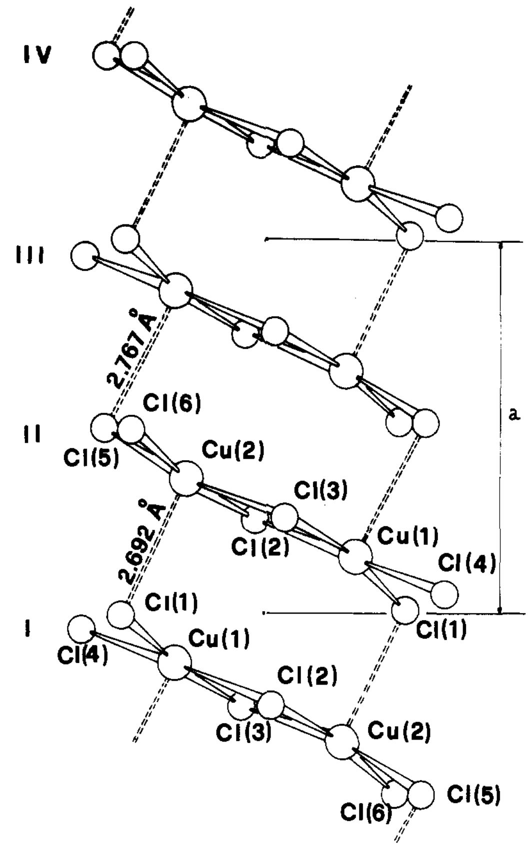

Figure 2. Stacking of $Cu_2Cl_6^{2-}$ units seen along the *b* axis.

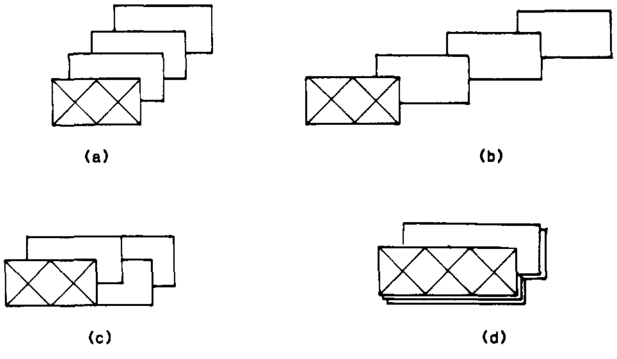

Figure 3. Stacking of $Cu_nCl_{2n+2}^{2-}$ oligomers: (a) in $KCuCl_3$;[16] (b) in $(CH_3)_2CHNH_3CuCl_3$;[17] (c) in $(melH_2)Cu_2Cl_6$ (this work); (d) in $[(C_2H_5)NH_2]_2Cu_4Br_{10} \cdot EtOH$.[18]

In addition, the packing of the dimers leads to a second, much longer Cu–Cl interaction between adjacent dimers [Cu(1)–Cl(2)$^{\mathrm{II}}$ = 3.021 Å, Cu(2)$^{\mathrm{II}}$–Cl(2)$^{\mathrm{III}}$ = 3.125 Å]. Since these distances are comparable to the distances between the least-squares planes, it seems appropriate to describe these as essentially nonbonded or at least very weakly bonded interactions. Thus it seems appropriate to specify this as 4 + 1-coordination (elongated square pyramidal) but to recognize that additional long interactions exist, which may be important magnetically.

The stacking of the $Cu_2Cl_6^{2-}$ dimers observed in this salt represents a new type not previously observed. In $KCuCl_3$ and NH_4CuCl_3, the stacking is uniform with an identical displacement, equal to the length of one Cu–Cl distance, between each pair of dimers (see Figure 3a).[16] In the low-temperature phase of $(CH_3)_2CHNH_3CuCl_3$[17] the stacking is again uniform, but with

---

(16) Willett, R. D.; Dwiggens, C.; Kruh, R. F.; Rundle, R. E. *J. Chem. Phys.* **1963**, *38*, 2429.

(17) Willett, R. D. *J. Chem. Phys.* **1966**, *44*, 39.

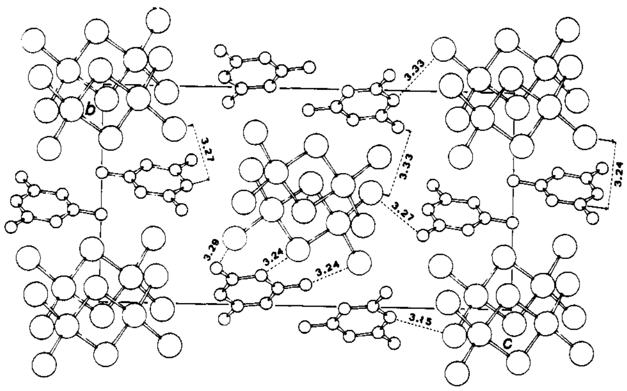

Figure 4. Molecular packing of diprotonated melamine–hexachlorodicuprate as seen along the *a* axis. For sake of clarity the Cu–Cl′ "long bonds" are omitted.

a larger displacement (Figure 3b). In this melamine salt the displacement alternates in the following manner (Figure 3c): each displacement is the length of one Cu–Cl distance, but the direction of the displacement alternates between the directions of the two terminal Cu–Cl bonds in the dimer. This yields a net displacement between next-nearest neighbors of one Cu–Cu distance. It is worth noting that the stacking of the $Cu_3Br_8^{2-}$ trimers in $[(C_2H_5)_2NH_2]Cu_4Br_{10}\cdot EtOH$[18] is such that displacements alternate between opposite directions of the same Cu–Br distance, so that next-nearest neighbors lie directly on top of each other (Figure 3d). The stacking, described in terms of the notation introduced in ref 3b, is specified by the symbols $2(^1/_2, ^1/_2)$ (Figure 3a), $2(^3/_2, ^1/_2)$ (Figure 3b), $2(^1/_2, ^1/_2)(^1/_2, -^1/_2)$ (Figure 3c), and $3(^1/_2, ^1/_2)(-^1/_2, -^1/_2)$ (Figure 3d).

It is also interesting to stress the "cis" configuration of the terminal chlorine atoms involved in the bonds between the dimers, because a "trans" configuration is shown by the chlorines linking $Cu_2Cl_6^{2-}$ dimers in chains in the analogous structure reported in literature.[19-21]

This is the first structural example reported of a noncentrosymmetric $Cu_2X_6^{2-}$ or $Cu_2X_4L_2$ dimer, the loss of the center of inversion being dictated by the stacking pattern. The bond distances within the dimer are normal, with the terminal Cu–Cl bonds (2.261 Å average) significantly shorter than the bridging Cu–Cl bonds (2.334 Å average).

Of interest magnetically are the bridging Cu–Cl–Cu angles within the dimer (95.8° average), which are very similar to those observed in other quasiplanar dimers.

The $Cu_2Cl_6^{2-}$ ions is to be considered planar. The most relevant deviations from the best least-squares plane are found for the two chlorine atoms linking the adjacent dimers (0.306 and –0.331 Å for Cl(1) and Cl(5), respectively). The loss of the center of symmetry in the dimer leads to the possibility of different extents of distortion at the two copper centers. In fact, the extent of distortion is small (not substantially larger than in $KCuCl_3$, for example[16]) and much smaller than in $(CH_3)_2CHNH_3CuCl_3$[17] or (4-bzpipdH)$CuCl_3$.[19]

The molecular geometry of the diprotonated melamine is as expected.

Figure 4 shows a projection along the *a* axis of the molecular packing. Note that the chlorine atoms of the anion are involved in the shortest intermolecular contacts not only with the nitrogen atoms of the triazine ring, but also with the carbon atoms (the shortest distances Cl–N and Cl–C are 3.15 Å and 3.24 Å, respectively). The closest distance between the nonbridging chlorines and the aminic nitrogens is 3.24 Å. In analogous compounds the formation of strong hydrogen bonds is evidenced when the contacts Cl–N are as short as 2.80 Å.[21,22] On the other hand examples of weaker hydrogen bonds greater than 3.2 Å are reported (see for example ref 23).

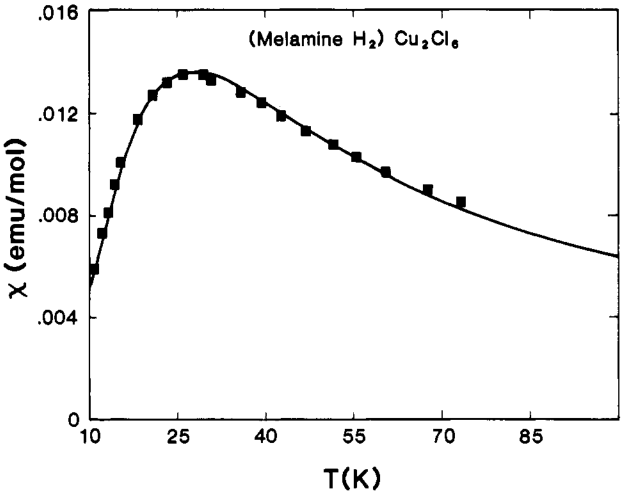

Figure 5. Magnetic susceptibility vs. temperature for $(melH_2)Cu_2Cl_6$. The solid curve is described in the text.

The lack of clearly defined electron density maxima near the expected hydrogen atom locations on the final difference Fourier map makes it impossible to draw conclusions concerning the sites of hydrogen atoms or the actual hydrogen bonding network. Also, no systematic variations occur in exocyclic or ring C–N distances, nor in a similar manner for the N–C–N angles, which makes it impossible to assign the sites of protonation. These facts may be due to a disorder of the hydrogen locations. Without addition information, it does not seem wise to speculate on the nature of the possible disorder at this time or on the presence of H bonding.

Spectroscopic Results. In agreement with the structural results, d–d band shapes and positions (9760 sh, 11 760 cm^{-1}) are very similar to those found in chlorocuprates(II) having distorted square-pyramidal or square-bipyramidal geometries.[19] Furthermore it presents a weakly intense band maximum at 19 610 cm^{-1}, which, being absent in monomeric complexes, is characteristic of dimeric or polymeric $Cu_2Cl_6^{2-}$ anions, independent of their coordination geometry.[17]

The complexity of the structure in our compound does not enable terminal Cu–Cl vibrations to be distinguished from bridging Cu–Cl vibrations. However, by comparison with chlorocuprates(II) having similar geometries[17] and support from literature data,[23-25] the bands appearing at 300, 284, and 266 (sh) cm^{-1} may be tentatively associated with the shortest equatorial Cu–Cl bonds and the band at 232 cm^{-1} with the longer axial Cu–Cl bond.

Magnetic Results. The high-temperature susceptibility of the compound obeys a Curie–Weiss law with $C = 0.91$ and $\Theta = -28$ K, indicative of a predominant antiferromagnetic interaction. At low temperatures, the presence of a weak paramagnetic tail is observed. This corresponds to a 2.4% monomeric impurity. When corrected for this impurity, χ effectively goes to zero as T approaches zero. Because of the complexity of the structure, it seems dangerous to postulate magnetic models. The structure consists essentially of an alternating chain of inequivalent dimers. Multiple-exchange pathways exist between dimers. Thus there exists one intradimer coupling (ΔE, the singlet–triplet splittings within the dimer) and a minimum of two intradimer exchange parameters, (J_1' and J_2') corresponding to the two exchange pathways between dimers, as well as mean field parameters, describing interchain interactions. This is clearly too large a set

---

(18) Fletcher, R.; O'Brien, S.; Bloomquist, R. D.; Hansen, J. J.; Willett, R. D. *Inorg. Chem.* **1983**, *22*, 330.

(19) Battaglia, L. P.; Bonamartini Corradi, A.; Marcotrigiano, G.; Menabue, L.; Pellacani, G. C. *Inorg. Chem.* **1980**, *19*, 125.

(20) Smith, D. W. *Coord. Chem. Rev.* **1976**, *21*, 93.

(21) Roberts, S. A.; Bloomquist, D. R.; Willett, R. D.; Dodgen, H. W. *J. Am. Chem. Soc.* **1981** *103*, 2603.

(22) Antolini, L.; Marcotrigiano, G.; Menabue, L.; Pellacani, G. C. *J. Am. Chem. Soc.* **1980**, *102*, 1203.

(23) Harlow, R. L.; Wells, W. J.; Watt, G. W.; Simonsen, S. H. *Inorg. Chem.* **1975**, *14*, 1768.

(24) Adams, D. M.; Lock, P. J. *J. Chem. Soc. A* **1967**, 620.

(25) Heyns, A. M.; Schutte, C. J. H. *J. Mol. Struct.* **1971**, *8*, 339.

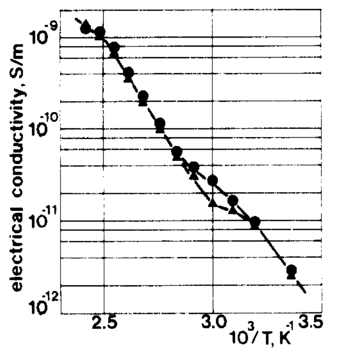

Figure 6. Isochronal [(circle) 1 min, (triangle) 10 min] electrical conductivity vs. reciprocal absolute temperature.

of parameters to determine uniquely from the susceptibility data.

Qualitatively, the data can be interpreted on the basis of the idea of a chain of dimers, e.g. an alternating linear chain system. The fact that χ goes to zero as T goes to zero shows that indeed some alternation does occur. For a simple antiferromagnetic alternating chain, the temperature at which χ reaches a maximum is essentially constant at $T_{\max} = 0.62\Delta E$, so we obtain $\Delta E/k \approx$ 45 K (Figure 5). As a first approximation, the data was fit to a simple dimer model with a paramagnetic impurity, as in eq 1,

$$\chi = (1-\alpha)\frac{C}{T}\,\frac{3\exp(-\Delta E/kT)}{1+3\exp(-\Delta E/kT)} + \alpha\frac{C}{T} \qquad (1)$$

where C is the Curie constant for the triplet state and α is the fractional dimer impurity. An excellent fit of the data was obtained over the full temperature range, with no systematic deviation of the fit from the data, with $C = 0.966$, $\Delta E/k = 43.7$ K and $\alpha = 0.0124$. Unfortunately the Curie constant corresponds to $g = 2.27$, which is unrealistically large. This indicates that substantial *ferromagnetic* coupling exists between dimers. The data for $T > 10$ K was fit to a mean field-corrected dimer model, yielding $C = 0.920$, $\Delta E/k = 53.8$ K, and $J/k = 7$ K (α fixed at 0.12) as shown by the solid line in Figure 5. This value of C corresponds to the more reasonable value of $g = 2.21$. These exchange parameters must be viewed as only approximate because of the mean field nature of the model, but results for more realistic models do not exist for coupling of ferromagnetic intradimers. In discussing magnetostructural correlation in copper(II) halides, two principle structural features have been recognized: the bridging Cu–Cl–Cu angle, Φ, and the extent of distortion of the dimer from planarity.[26] The effect of increasing Φ is to make the exchange interaction more antiferromagnetic. Conversely, distortions from planarity tend to make the coupling more ferromagnetic. In addition there is evidence that decreasing the number of axial ligands increases the antiferromagnetic contribution.[27] This is reasonable since EPR results indicate more delocalization of the unpaired electron out onto the chloride ions. In this salt, the distortions of the dimer are small, so we expect the dominant factor to be the bridging angle. Thus we can compare the parameters for the melaminium salt ($\Phi = 95.8°$, $2J/k = -54$ K) with those for the $Cu_2Cl_4^{2-}$ dimer, in $KCuCl_3$ ($\Phi = 95.9°$, $2J/k = -55$ K).[27] Thus, in these two salts, where the principle coordination is essentially planar, the exchange-coupling parameters are identical. On the other hand, the salts (*n*-methyl-2-aminopyridinium)$CuCl_3$, with $n = 4$ and $n = 6$ (hence 4MAPC and 6MAPC), have recently been studied.[28] These are one-dimensional systems with symmetric dibridged chains of square-pyramidal copper(II) ions. The results for 4MAPC ($\Phi = 94.3°$, $2J/k = -86$ K) and 6MAPC ($\Phi = 95.3°$, $2J/k = -110$ K) indicate the presence of much stronger antiferromagnetic coupling. Conversely, a series of $ACuCl_3$ salts exist that contain one-dimensional chains of dimers with stacking identical with, or closely related to, that depicted in Figure 3b.[26,29] Here a 4 + 1-coordination exists with coordination geometry sometimes described as intermediate between an elongated square pyramid and a trigonal bipyramid. Here, in this series of dimers a nearly constant bridging angle, the exchange coupling becomes increasingly ferromagnetic as the distortion increases: A = $(CH_3)_2CHNH_3^+$ ($\Phi = 95.5°$, $2J/k = -25$ K), A = $(CH_3)_2NH_2^+$ ($\Phi = 95.6°$, $2J/k = 28$ K), A = 4-benzylpiperidinium ($\Phi = 95.3°$, $2J/k = 60$ K). Thus the magnetic data support the argument that the copper coordination is best described as square planar with weaker axial interactions.

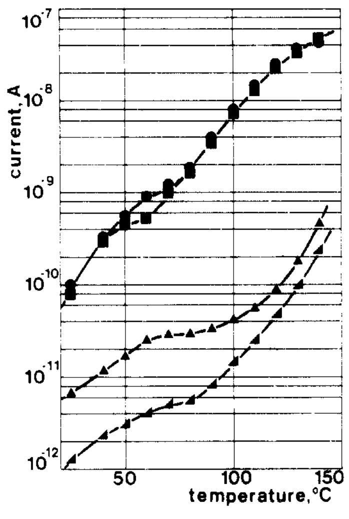

Figure 7. Isochronal charging [(circle) 1 min, (square) 10 min] and discharging [(regular triangle) 1 min, (slanted triangle) 10 min] currents vs. temperature.

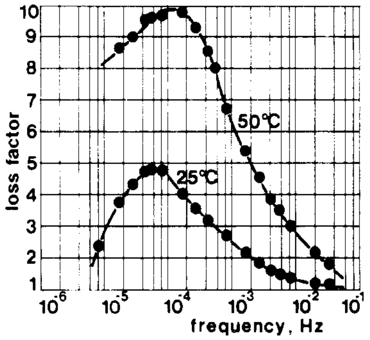

Figure 8. Loss factor as function of frequency and temperature.

Electrical Properties. The electrical conductivity calculated at 1 and 10 min from the application of the voltage plotted in Figure 6 as a function of reciprocal absolute temperature exhibits an almost linear behavior, particularly above 60 °C for the 10-min values. The slope is rather low and corresponds to an apparent activation energy value of conduction of 0.34 eV. The room temperature value of electrical conductivity is 2.8×10^{-12} S/m, which classifies the compound as an insulator. At 60 °C, an evident current transient takes place; the same can be seen in the isochronal charging and discharging currents at 1 min, plotted in Figure 7 as functions of temperature, and in isothermal charging and discharging currents as functions of time (not shown).

Dielectric measurements in the frequency range 10^{-2}–10^{6} Hz do not show noticeable effects in the same temperature range of Figures 6 and 7. The relative dielectric constant regularly decreases with frequency, reaching the value of 6.2 at 1 kHz and room temperature; this value is approximately constant for frequencies up to 1 MHz. The loss factor regularly decreases with frequency up to very small values of about 0.03 at room temperature, thus confirming again the insulating nature of the

---

(26) Willett, R. D. In "Magneto-Structural Correlations in Exchange Coupled Systems"; Willett, R. D., Gatteschi, D., Kahn, O., Eds.; Reidel: Dordrecht, The Netherlands, 1984.

(27) Maass, G.; Gerstein, B. C.; Willett, R. D. *J. Chem. Phys.* **1967**, *46*, 401.

(28) Geiser, U.; Willett, R. D. *J. Appl. Phys.* **1984**, *55*, 2407.

(29) O'Brien, S.; Gaura, R. M.; Landee, C. P.; Willett, R. D., to be submitted for publication.

Inorg. Chem. **1985**, *24*, 2905-2910

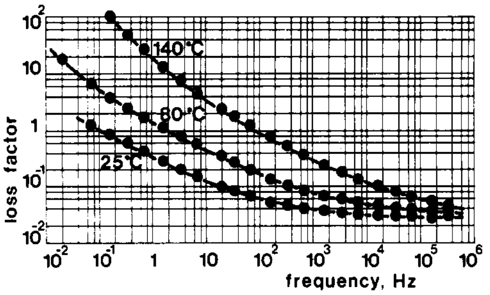

Figure 9. Loss factor vs. frequency from isothermal dc data.

compound. On the contrary, the loss factor increases to very high values with decreasing frequency and increasing temperature, as can be seen in Figure 8. The tendency of the slope to unity for the highest temperature (140 °C) and frequencies below 10 Hz is noteworthy. The low value of the apparent activation energy of conduction and the dielectric absorption increasing with increasing temperature and decreasing frequency, with the slope approaching unity at 140 °C, point out an ionic mechanism of conduction.[11,30-33] The same is supported by the relaxation phenomenon found below ~10^{-2} Hz by the Hamon treatment of the isothermal dc data,[9-11] as can be seen in Figure 9. This relaxation process is temperature activated and may be ascribed to polarization effects of the Maxwell-Wagner-Sillars type due to crystal interfaces in these polycrystalline samples.[31-33]

Charge carriers might be identified in protons coming from hydrogen bonding of molecules in the material, according to the stacking of molecular units in the crystals. The conduction transiton near 60 °C could arise from molecular phenomena associated with proton dissociation and hopping in crystal lattice.

Conclusions. Our dimeric copper(II) chloride salt exhibits a new stacking pattern previously not observed in copper oligomers. The direction of displacements alternates as one progresses along the stack, leading to a net displacement always parallel to the Cu-Cu direction. The coordination geometry of the Cu(II) ions in the noncentrosymmetric $Cu_2Cl_6^{2-}$ dimers is probably best described as distorted square pyramidal (4 Cu-Cl = 2.3 Å; 1 Cu-Cl = 2.7 Å).

Magnetically, the system behaves as a chain of ferromagnetically coupled antiferromagnetic ($S = 0$ ground state) dimers. The intradimer interaction of $\Delta E/k = 54$ K is consistent with the results of other $Cu_2Cl_6^{2-}$ dimers that are nearly planar and have net antiferromagnetical coupling between the copper ions. Detailed analysis of the magnetostructural correlations is not possible due to the complexity of the structure and to the approximate nature of the magnetic analysis. Finally, the material behaves as an electrical insulator whose small dc conductivity is explainable[6] on the basis of an ionic mechanism of conduction while dipolar relaxation processes do not appear to be meaningful. The principal charge carriers seem to be the protons associated with the hydrogen network in the crystal, which arises from molecular stacking in the crystals.

Acknowledgment. This work was supported in part by NSF Grants DMR-8219430 and INT-8219425 and in part by a contribution of the Ministero della Pubblica Istruzione of Italy. The assistance of Professor C. P. Landee with the magnetic data collection is gratefully acknowledged.

Registry No. (melH$_2$)Cu$_2$Cl$_6$, 94007-98-4.

Supplementary Material Available: Listings of the thermal parameters for the atoms of the title complex, observed and calculated structure factors, torsion angles for the $Cu_2Cl_6^{2-}$ anion chain, and deviations of atoms from least-squares planes and TG and DSC figures (26 pages). Ordering information is given on any current masthead page.

---

(30) Link, G. L. In "Polymer Science"; Jenkins, A. D., Ed.; North Holland: London, **1972**; Vol. 2, p 1281.
(31) Kryszewsky, M. *J. Polym. Sci., Polym. Symp.* **1975**, *50*, 359.
(32) Blythe, A. R. "Electrical Properties of Polymers"; Cambridge University Press; Cambridge, England, 1979.
(33) Seanor, D. A. "Electrical Properties of Polymers"; Academic Press: New York, 1982.

Contribution from the Departments of Chemistry, North Carolina State University, Raleigh, North Carolina 27695-8204, and The University of North Carolina at Chapel Hill, Chapel Hill, North Carolina 27514

Synthesis and Coordination Chemistry of a New 1,2-Dithiolene Containing the Tetrathioethylene Unit[†]

CHARLES T. VANCE,[‡] ROBERT D. BEREMAN,*[‡] JON BORDNER,[‡] WILLIAM E. HATFIELD,[§]
and JEFFERY H. HELMS[§]

Received October 11, 1984

The synthesis and characterization of a new 1,2-dithiolene ligand, the dipotassium salt of 5,6-dihydro-1,4-dithiin-2,3-dithiolate (DDDT), are reported. This salt reacts with Ni(II) in methanol to yield the apparent Ni(III) product, Ni(DDDT)$_2^-$, which was isolated as the tetraethylammonium salt. A single-crystal structural study on this complex was carried out. Crystals belong to the monoclinic space group $C2/c$ with $a = 22.297$ (4) Å, $b = 8.152$ (1) Å, $c = 17.103$ (3) Å, $\beta = 129.31$ (1)°, $R = 5.1\%$ for 1168 reflections, and ρ(calcd) = 1.518 ρ(obsd) = 1.52, for $Z = 4$. The structure was solved by a combination of Patterson, Multan, Fourier, and least-squares techniques. The Ni atoms are located on crystallographic centers of symmetry. The average Ni-S distance of 2.148 (2) Å is very close to those of other monoanionic nickel dithiolenes. Single-crystal ESR data gave the principal g value assignments of $g_{zz} = 2.022$ (1), $g_{xx} = 2.057$ (1), and $g_{yy} = 2.119$ (1). A solution and frozen-glass ESR study of the ^{61}Ni-enriched complex yielded the hyperfine splitting values (in gauss) of $\langle A \rangle_0 = 4.5$, $A_{zz} < |0.2|$, $A_{yy} = |2.4\ (3)|$, and $A_{xx} = |14.2\ (3)|$. A variable-temperature magnetic study showed antiferromagnetic behavior ($J = -8.5$ cm^{-1}) with long-range magnetic ordering below 15 K. The structural data, ESR data, and magnetic data when taken together support a highly delocalized π HOMO.

Introduction

Over the past 10 years, the organic chemistry of sulfur has been highly influenced by the unique physical properties of tetrathiafulvalene (TTF).[1-4] The early proposal by Wudl[5] and others that the TTF framework might yield the prerequisite properties necessary to yield an "organic metal", coupled with the recent findings that bis(tetramethyltetraselenafulvalenium) perchlorate is a superconductor at 1 K,[6] has further increased the interest in

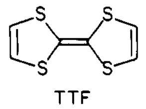

TTF

[†] Coordination Chemistry of New Sulfur Containing Ligands. 27.
[‡] North Carolina State University.
[§] The University of North Carolina at Chapel Hill.

(1) Narita, M.; Pittman, C. U., Jr. *Synthesis* **1976**, 489.
(2) Kaplan, M. L.; Wudl, F.; Haddon, R. C.; Hauser, J. J. *Chem. Scr.* **1980**, *15*, 196.

0020-1669/85/1324-2905$01.50/0